

An AFM-SEM investigation of the effect of silica fume and fly ash on cement paste microstructure

V. G. PAPADAKIS*, E. J. PEDERSEN

Danish Technological Institute, Building Technology Division, Concrete Centre, Gregersensvej, P.O. Box 141, DK-2630 Taastrup, Denmark
E-mail: *vagelis.g.papadakis@dti.dk*

H. LINDGREEN

Geological Survey of Denmark, Thoravej 8, DK-2400 Copenhagen NV, Denmark

Atomic force microscopy (AFM) was used to observe particle shape and surface texture details of normal portland cement and supplementary cementing materials (silica fume, low-calcium fly ash, and high-calcium fly ash). The latter materials mixed with cement were examined after prolonged hydration. Significant innovative information on particle shape and hydrated paste microstructure was obtained. Conventional microscopy techniques, such as scanning electron microscopy (SEM), cannot provide such detailed images and surface texture characteristics of the fine materials (especially silica fume) and of the product microstructure. AFM showed, for the first time, that silica fume particles are primarily composed of two complimentary parts (hemispheres or semicylinders). Nano-size particles were found in all materials. A relatively smooth product surface was observed in the hydrated cement paste. The hydrated surface of the addition-cement pastes presented small spheroid bulges, giving an additional roughness as was measured by AFM. A sufficient correlation of this microscopical quantitative information with macroscopical engineering and durability properties of cement products is also presented.

© 1999 Kluwer Academic Publishers

1. Introduction

For technical and economic reasons, new materials with pozzolanic and cementitious properties have been mixed with cement during the last years [1, 2]. Among these materials are industrial by-products such as fly ash from coal-burning electric power plants, slags from metallurgical furnaces, silica fume (or microsilica) from electric arc furnaces producing silicon and ferrosilicon alloys, and some naturally active materials such as volcanic tuffs. Their activity is mainly due to the reaction of their active constituents with $\text{Ca}(\text{OH})_2$ produced from cement hydration (pozzolanic activity) and the formation of hydrated products with binding properties. The exact structure and chemical formula of these products are still unknown.

The detailed knowledge of cement paste microstructure is of great importance for the understanding and prediction of cement applications' performance [3–5]. Visual examination, optical microscopy, and scanning electron microscopy (SEM) have been extensively used in microstructure research of hardened cement paste and concrete, providing additional understanding of macroscopical properties [1–5]. Electron microprobe analysis studies of hardened cement pastes have contributed to the compositional characterization of

hydration products and spatial information [6]. Transmission energy microscope (TEM) enables the identification and analysis of features on a significantly sub-micrometre scale [7]. However, these techniques most commonly investigate specimens under high vacuum, and thus alteration or damage on microstructure morphology may occur. Furthermore, some of these materials, such as silica fume, with a grain size distribution in the 0.02 to 0.3 μm range, are too small to be observed in detail by SEM. Techniques with stronger magnification capabilities would be very useful in these cases, as well in the better conception of the pure cement paste microstructure.

By atomic force microscopy (AFM) [8, 9], a sharp tip is scanning over a sample surface and three-dimensional images having resolution at nanometer level are obtained at atmospheric conditions (room temperature, humidity, and ambient pressure). AFM has been used to produce atomic resolution images of both conductors [10] and nonconductors [11, 12]. In the present decade, AFM has also been used in the study of cement surface microstructure, especially because surfaces can be imaged under aqueous solutions at normal conditions [13]. AFM has been applied to investigate the surface of alite alone and of alite covered with

* To whom correspondence should be addressed.

an organic admixture and has shown that the surface roughness of the alite decreased markedly after reaction with the organic admixture [14]. AFM was also used to investigate the early period of portland cement hydration, and a membrane/osmosis model was proposed [15]. A combination of nuclear magnetic resonance (NMR) and AFM showed that the hydration rate is highly correlated with the roughness of the gel surface [16]. For fly ash particles, AFM showed two types of spheres, dark, large ones (approximately 100 μm) with numerous craters on their surface and clear, small ones (approximately 10 μm) with smooth surface [17].

In the present work, AFM was used to observe particle shape and surface texture details of cement, silica fume, fly ashes, and hydrated mixtures. Distinct micrographs of 1 $\mu\text{m} \times 1 \mu\text{m}$ were taken, providing information on the particle shape of the additions and microstructure of the hydrated mixtures. The same materials were examined under SEM to obtain a general overview, and the comparative use of these two methods (SEM–AFM) is discussed. Finally, the correlation between the microstructure and the macroscopical engineering and durability properties of cement products is discussed.

2. Experimental procedure

2.1. Materials and sample preparation

Three typical cementitious and/or pozzolanic additions were examined; a silica fume, a low-calcium fly ash, and a high-calcium fly ash. The silica fume (SF) originated from Norway (Elkem Materials A/S, Kristiansand) and is a typical highly pozzolanic material. The low-Ca fly ash (FL) was produced in Denmark (distributed by Danaske I/S, Aalborg) and is categorized as normal pozzolanic material. The high-Ca fly ash (FH) was produced in Greece (Public Power Corporation, Ptolemais) and is a cementitious mineral admixture. Thus, the choice of these materials covers almost all the range of cementitious–pozzolanic by-products used in concrete. SF and FL were used as they were delivered from the producers, whereas FH was pulverized prior to use, to meet the FL mean particle size. A normal portland cement (350 m^2/kg Blaine's fineness) was used.

The main physical properties and chemical analyses of the materials are given in Table I. Particle size distribution of the materials, determined by X-ray sedimentation technique, showed that the mean particle diameter of fly ashes was 13 μm , similar to the cement particles. SF particles, as reported in the literature [1], are about 100 times smaller in size (0.1 μm average diameter).

Four paste specimens were cast in small plastic containers. The pastes were made of normal portland cement (control), cement plus 10% silica fume, cement plus 20% low-calcium fly ash, and cement plus 20% high-calcium fly ash. A water-to-cement ratio (W/C) of 0.5 was retained for all pastes. First, the cement amount (10 g) was added and then the corresponding amount of the additive. These materials were mixed by hand for two min; then the corresponding amount (5 g) of the water was added and the fresh paste was further mixed

TABLE I Main physical and chemical characteristics of normal portland cement, silica fume (SF), low-calcium fly ash (FL), and high-calcium fly ash (FH)

| | Cement | SF | FL | FH |
|---|--------|-------|-------|-------|
| Physical Properties | | | | |
| Mean diameter, μm | 14.0 | 0.36 | 13.3 | 12.6 |
| BET surface area, m^2/g | 1.1 | 18 | 1.2 | 6.2 |
| Density, kg/m^3 | 3,160 | 2,260 | 2,250 | 2,660 |
| Chemical Analysis, % | | | | |
| SiO ₂ | 20.12 | 90.90 | 53.50 | 39.21 |
| Al ₂ O ₃ | 4.25 | 1.12 | 20.40 | 16.22 |
| Fe ₂ O ₃ | 3.49 | 1.46 | 8.66 | 6.58 |
| CaO | 63.20 | 0.69 | 3.38 | 22.78 |
| Free CaO | 1.48 | 0.024 | 0.36 | 5.18 |
| MgO | 1.26 | 0.77 | 2.25 | 2.35 |
| SO ₃ | 2.88 | 0.38 | 0.60 | 4.30 |
| Loss on ignition | 0.86 | 3.00 | 2.20 | 2.10 |
| Other Characteristics | | | | |
| Insoluble Residue, % | 0.14 | 62.85 | 78.4 | 30.88 |
| Glass Phase, % | — | 96 | 75 | 50 |

for 2 min. One day after the casting, 1 ml of water was added to all specimens. The containers were hermetically sealed and placed at 20 °C constant temperature. Microscopy analyses were performed after six months.

2.2. Atomic force microscopy

Material particles and paste samples were examined by atomic force microscope (RasterscopeTM 4000, Danish Micro Engineering A/S) running in noncontact mode (0.1 nN force). The particles in the cement, silica fume, and fly ashes were dispersed by ultrasonic treatment; the silica fume in distilled water and the other components in acetone in order to avoid hydration. The specimens were prepared by leaving one drop of the suspension to dry at room conditions on a block of highly oriented pyrolytic graphite (HOPG). The samples from the pastes were removed by hammer stroke from the paste specimens, oven-dried at 105 °C for 24 h. Small pieces of material were then glued onto AFM sample holders and slightly polished in dry condition. All specimens were examined at room conditions (~20 °C, 1 atm and 40–60% relative humidity).

2.3. Scanning electron microscopy

All of the above particles and pastes were also examined by means of scanning electron microscope (LEO 435 VP). Surface micrographs of 8,000 magnification size were obtained and can be used as a general overview of the materials.

3. Results and discussion

3.1. Cement, silica fume, and fly ash particles

Typical SEM micrographs of cement and additions are presented in Fig. 1 and AFM micrographs in Figs 2–5.

As observed by SEM (Fig. 1a), cement particles have an irregular polygonal shape. Particle sizes range from 15 to less than 0.5 μm . From AFM (Fig. 2), some

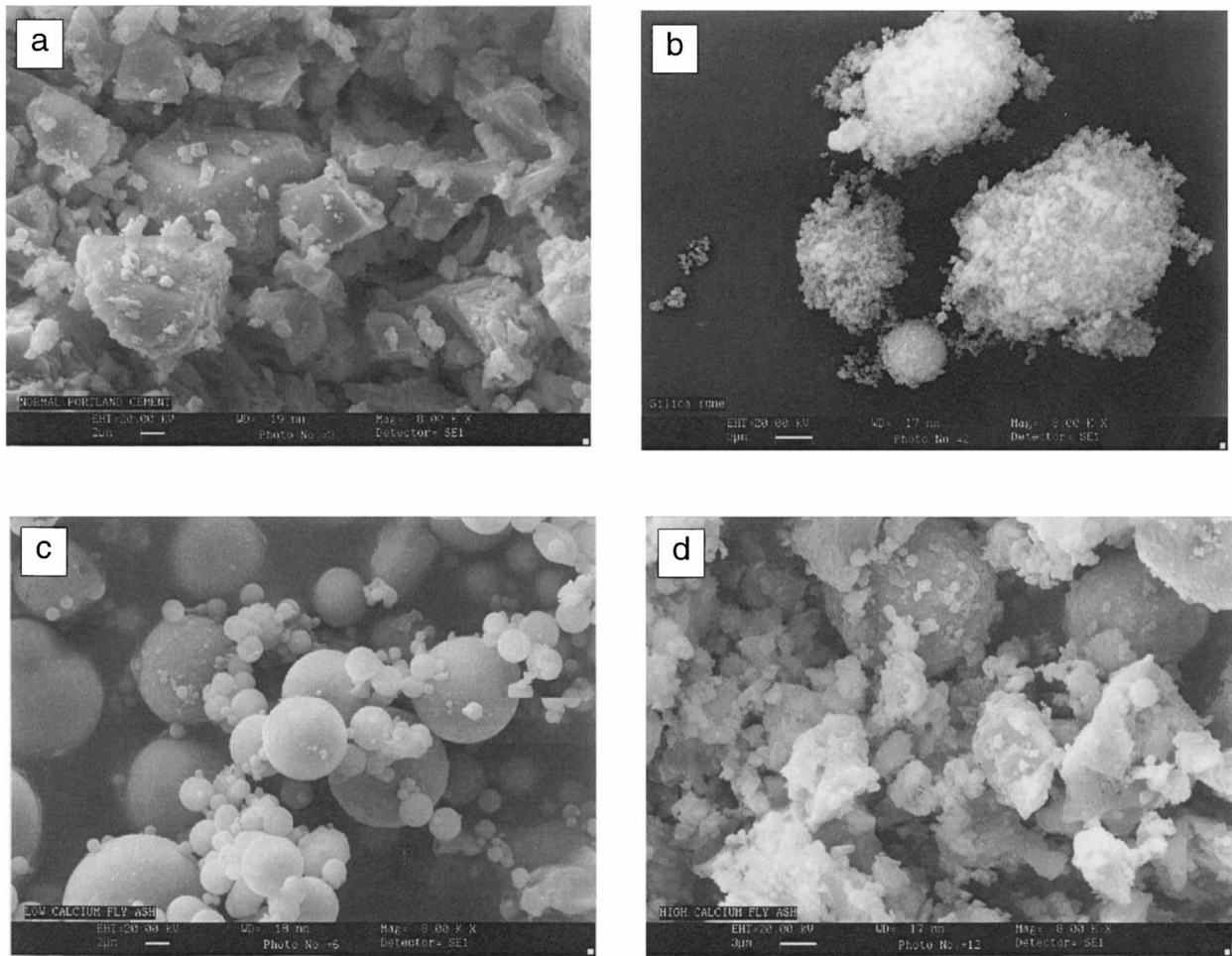


Figure 1 SEM micrographs: (a) normal portland cement, (b) silica fume, (c) low-calcium fly ash, and (d) pulverized high-calcium fly ash.

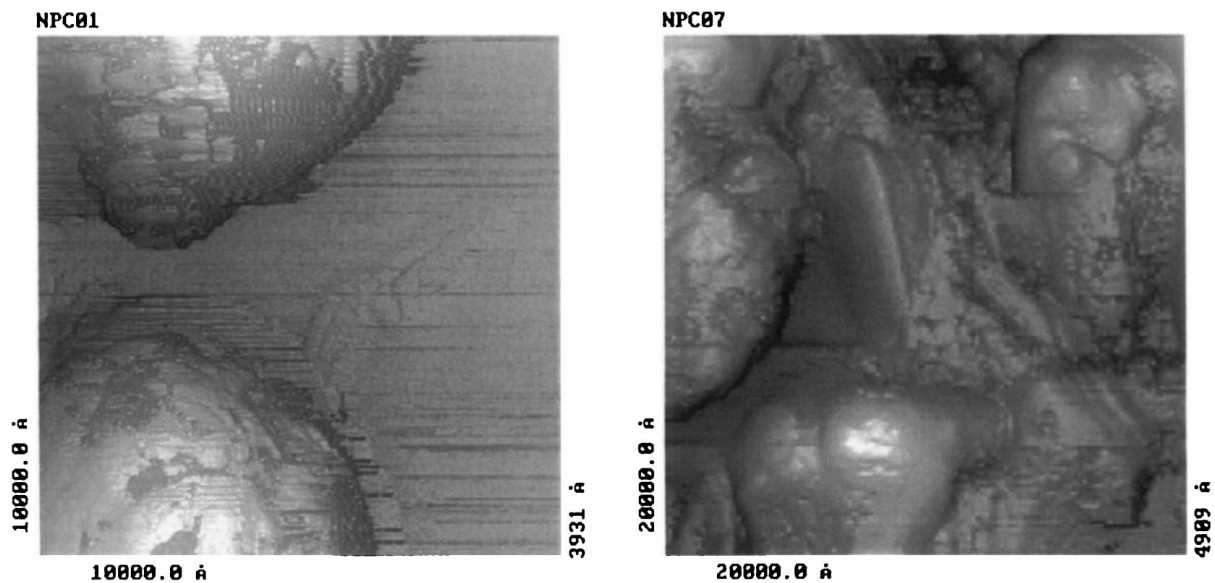


Figure 2 AFM micrographs of normal portland cement particles.

particles of size 1 to 0.5 μm in diameter are rounded, with a globular surface, whereas others are polygonal. However, some irregular particles of size less than 0.1 μm in diameter were observed (Fig. 2, right).

Silica fume particles are too small in size to be imaged in detail by SEM (Fig. 1b). From AFM (Fig. 3), the silica fume investigated has particle diameters of about 0.1 μm , in agreement with previous reported dimen-

sions [1]. Two particle shapes are present, one spheroidal and one cylindrical. It is very characteristic of the material that all particles are composed of two complementary parts (hemispheres or semi-cylinders). This feature can be explained from the production of silica fume, where the reduction of quartz to silicon at about 2000 $^{\circ}\text{C}$ produces a gaseous SiO , which is transported to lower temperatures, where it is oxidized and condensed [1].

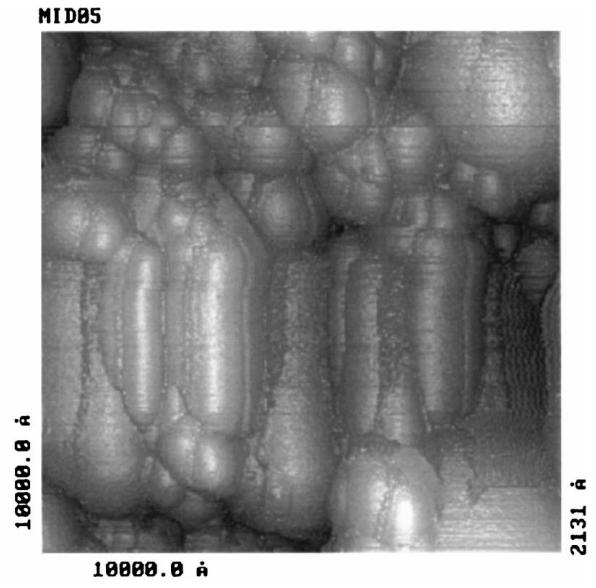
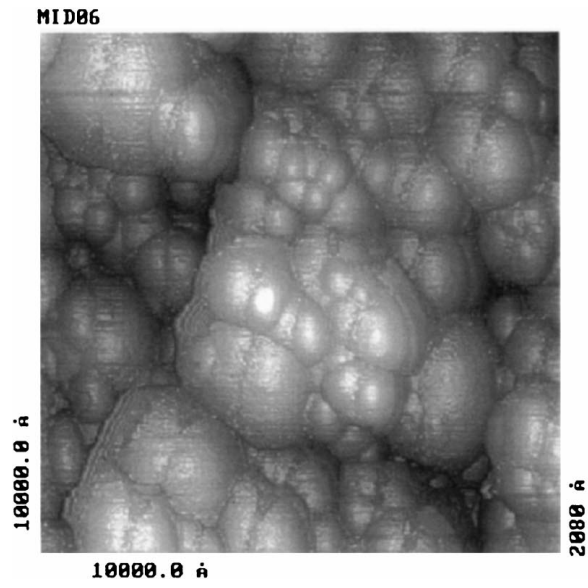


Figure 3 AFM micrographs of silica fume particles.

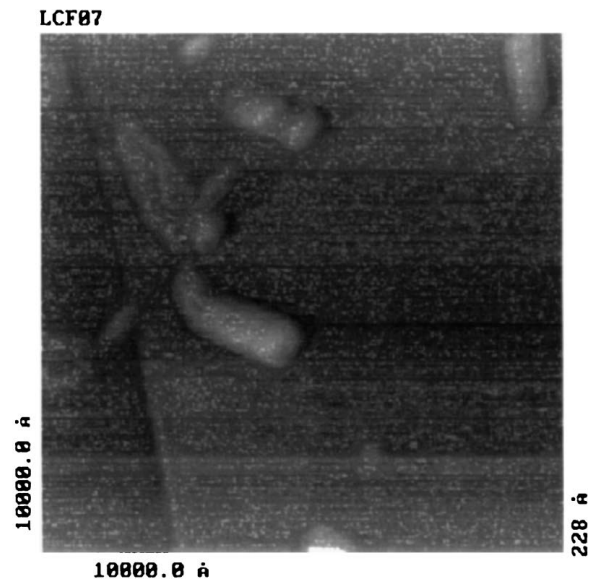
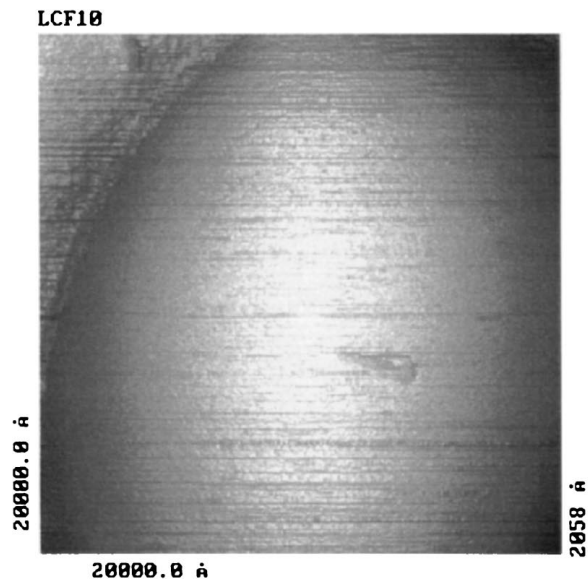


Figure 4 AFM micrographs of low-calcium fly ash particles.

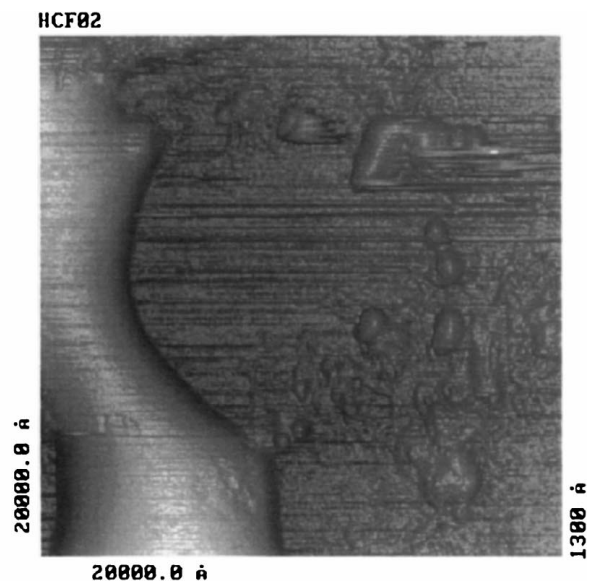
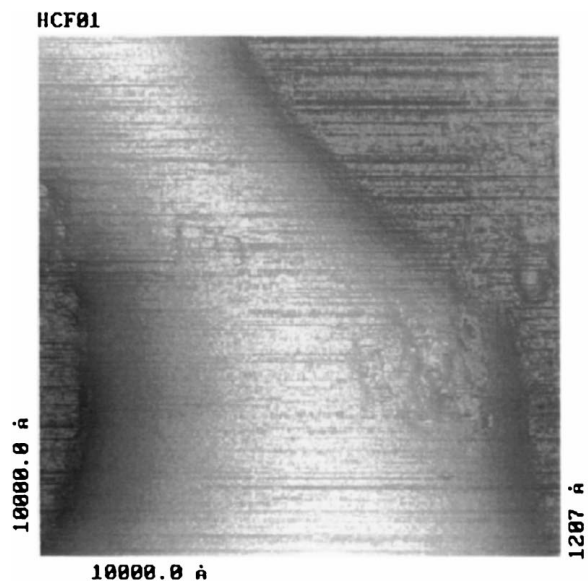


Figure 5 AFM micrographs of high-calcium fly ash particles.

This particular shape can help in SF identification in cement paste during the hydration process.

In general, fly ashes consist of glassy spheres of various sizes. Due to the lower proportion of surface deposits consisting of alkali sulphate crystals [18], FL tends to show a cleaner appearance in SEM (Fig. 1c). For the FH, many of the particles are perospheres containing numerous smaller particles, but after grinding, smaller size particles are produced having an irregular shape like the cement particles (Fig. 1d). Using AFM technique, it is observed (Fig. 4) that the FL consists primarily of large spheroid particles (approximately $3\ \mu\text{m}$) with a smooth surface, like found previously [17], and of smaller (in one dimension $< 0.1\ \mu\text{m}$) irregular shaped particles, reported for the first time. The FH (Fig. 5) consists of smooth, irregularly shaped particles, some too large to be seen by AFM, others much smaller (about $0.1\ \mu\text{m}$ in one dimension). These nano-size particles may be correlated with the early pozzolanic activity of the fly ashes.

3.2. Paste microstructure

SEM micrographs for all mature pastes are summarized in Fig. 6. In the control sample, very large $\text{Ca}(\text{OH})_2$ (CH) crystals and a porous composite mass of calcium silicate hydrate (CSH) and monosulphate are observed (Fig. 6a). In the SF-cement paste, the CH has been com-

pletely converted, and a very dense structure of CSH and monosulphate has been formed (Fig. 6b). Because of the significant pozzolanic reaction during the period of six months, the fly ash particles are difficult to identify, as they are covered by the reaction products (Fig. 6c and d). Few entire round particles are still distinguished. Similarly, for the fly ash-cement mixtures, a very dense structure has been formed comparing to the control.

AFM micrographs for the corresponding pastes are shown in Figs 7–10. The roughness (R_a) of the area was calculated on the slope corrected image $\{(X_i, Y_j, Z_{ij}); i = 1, 2, \dots, N; j = 1, 2, \dots, M\}$:

$$R_a = \frac{1}{N} \frac{1}{M} \sum_{i=1}^N \sum_{j=1}^M |Z_{ij} - Z_m|$$

where,

$$Z_m = \frac{1}{N} \sum_{i=1}^N Z_i$$

For the control paste, the roughness is 760, for the SF paste 960, for FL paste 940, and for the FH paste 450 (mean values of ten random measurements). The control paste has rather large grains with a rough surface, sometimes with angular faces (calcium hydroxide crystals), and with pores in between, and sometimes a

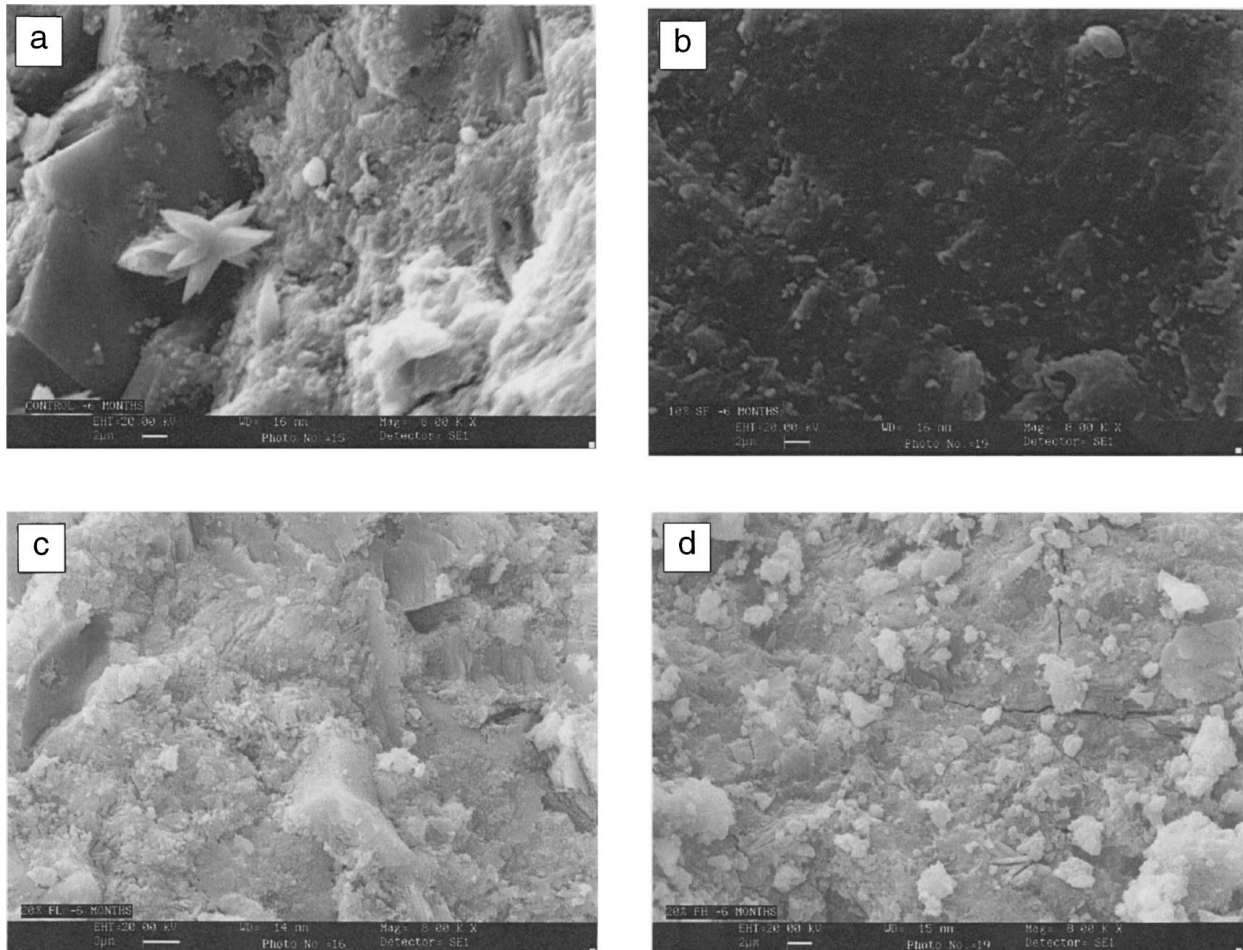


Figure 6 SEM micrographs: (a) hardened cement paste, (b) 10% SF-cement paste, (c) 20% FL-cement paste, and (d) 20% FH-cement paste, after six months of hydration.

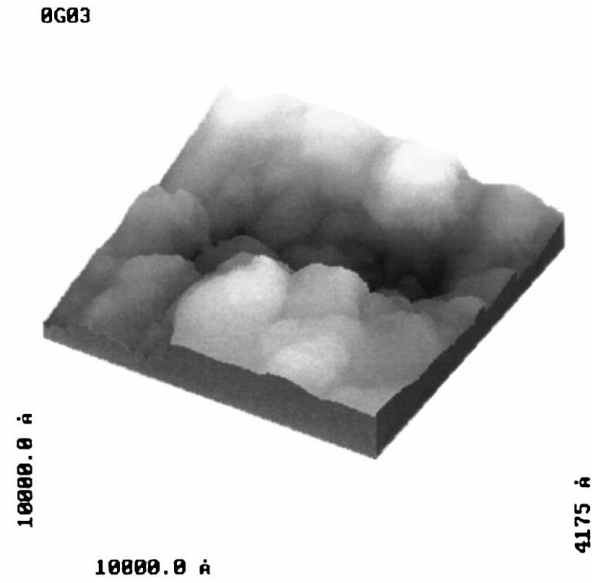
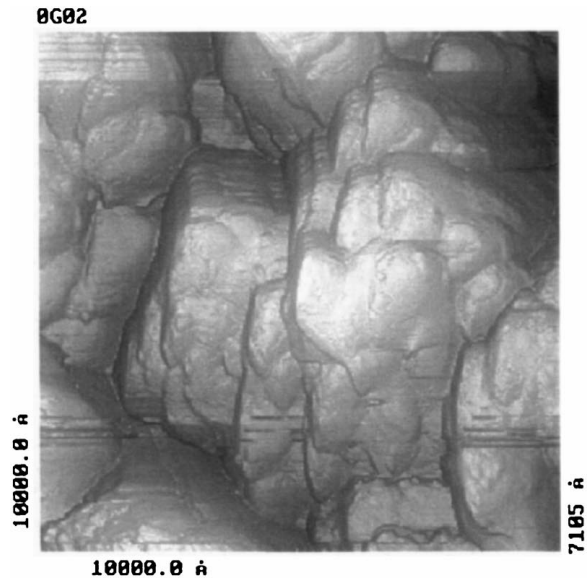


Figure 7 AFM micrographs of cement paste section after six months of hydration.

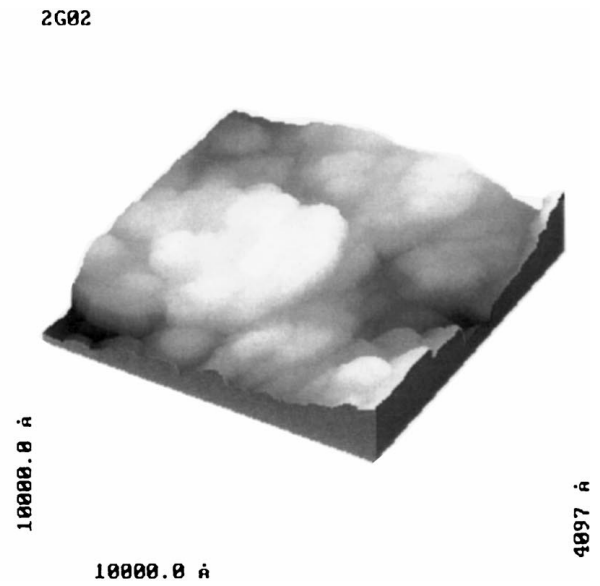
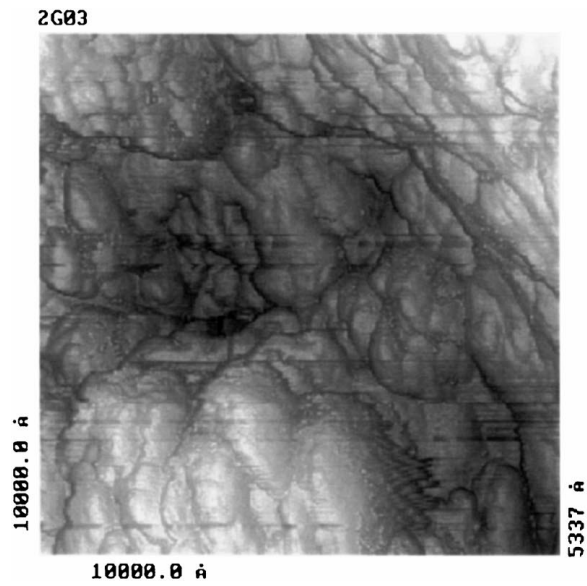


Figure 8 AFM micrographs of 10% SF-cement paste section after six months of hydration.

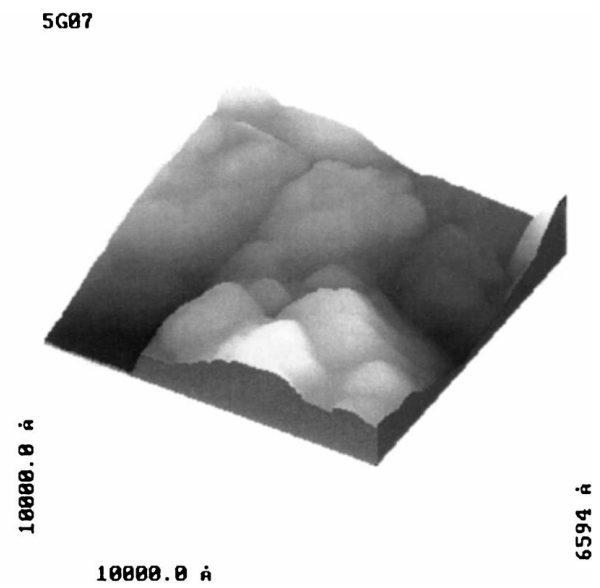
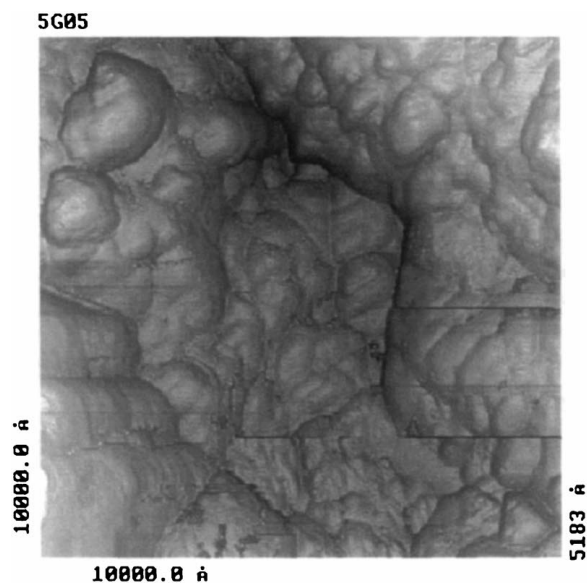


Figure 9 AFM micrographs of 20% FL-cement paste section after six months of hydration.

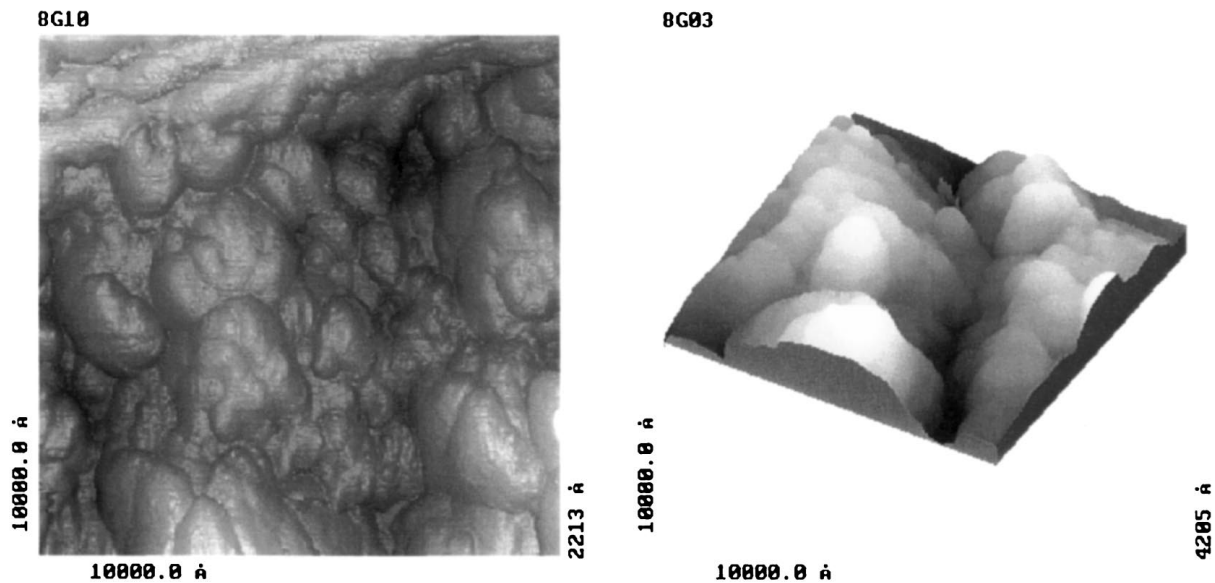


Figure 10 AFM micrographs of 20% FH-cement paste section after six months of hydration.

rather smooth surface intersected by slit-shape pores (Fig. 7). The SF paste has large smooth particles and filled pore spaces in which partly-reacted silica fume particles can be identified (Fig. 8). The fly ash pastes similarly have smooth particles and filled pore spaces in between (Figs 9, 10). Despite having a rough surface compared to the cement paste, the silica fume paste and the FL paste, the FH paste resembles the pure cement paste in having pores along particle boundaries, see for example, Fig. 10 (right).

3.3. Macroscopical properties

In order to examine the dependence of concrete macroscopical properties on cement paste microstructure, measurements of main engineering and durability properties were carried out. For this purpose, mortar specimens containing the above pastes were prepared. Normal graded sand was used as aggregate. The aggregate-to-cementitious materials (cement plus silica fume or fly ash) ratio was 3 for all specimens. Thus, additions are supposed to replace aggregate in the unit mortar volume. Preparation and experimental details are given elsewhere [19]. The specimens were tested after six months of hydration for modified cube compressive strength, total pore volume (gravimetric method using water), and chloride permeability (AASHTO test T 277-831).

In Fig. 11, the relative values of these characteristics for the addition-containing mortars regarding the control are presented. As can be observed, strength is improved by 25% for all cases of addition. This can be connected with the higher content of CSH and the more complicated product microstructure, as was observed in the AFM micrographs. Total pore volume was found almost the same for all mortars. This means that the pozzolanic reactions do not cause significant expansion on product volume.

However, despite the almost same porosity, addition-containing mortars presented much lower permeability

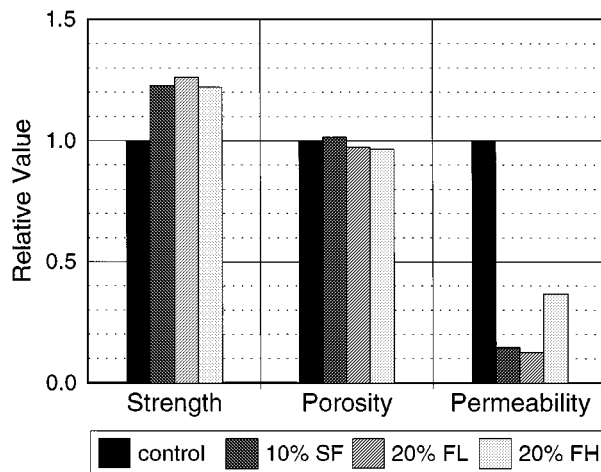


Figure 11 Macroscopic properties of cement-addition mortars after six months of hydration.

as compared to the control. Similarly, the specific surface area of the pure cement paste was significantly larger than the specific surface areas of the pastes with silica fume or fly ash ($28 \text{ m}^2/\text{g}$ for the pure cement compared to $20 \text{ m}^2/\text{g}$ for the SF and $19 \text{ m}^2/\text{g}$ for the fly ash pastes). This can be due to pore refinement (transformation of a system containing larger pores into one with smaller pores) and grain refinement (transformation of larger crystals, such as calcium hydroxide, into smaller crystals [18]). This filling of pores and spaces between larger particles was confirmed by AFM, but could not be related to roughness, which includes both spaces between particles and the roughness of single particle surfaces. The pore refinement and the consequent lower permeability observed for addition-containing pastes can retard deterioration phenomena [20] and elongate construction service lifetime.

4. Conclusions

SEM gives a sufficient general overview of particle shape in the case of relatively coarse materials (cement

and fly ashes), which is necessary for evaluation of the heterogeneity of the larger particles. AFM gives significant information on the shape of the fine part of these materials and especially on silica fume particle shape and surface texture. Silica fume particles were found to be mostly spheroid but cylindrical as well in shape, with 0.1 μm average diameter, and consisting primarily of two complimentary hemispheres or semi-cylinders.

For the pastes, SEM provided a general overview of the surface texture. By AFM, a detailed image of the product and pore microstructure was obtained. The pure cement paste has a variable surface intersected by pores, the surface sometimes being smooth and sometimes with angular particles having a rough surface. The internal surface of the addition-cement pastes presents small spheroid bulges giving an additional roughness. These bulges are particles of the additions that have reacted with calcium hydroxide. The texture of the pore walls is also clear, and the deposit of the addition-cement products in the pore space is obvious.

The pore and grain refinement supported by AFM are responsible for the strength and durability enhancement. All of these observations can be very useful both in practice for high durability and performance cement applications, and in the fundamental modeling of the additions activity in cement and concrete.

Acknowledgements

The European Commission, DG XII, provided financial support for this work, through the Training & Mobility of Researchers (TMR) Programme (Marie Curie Research Training Grant: ERBFMBICT961387). The Danish Technological Institute (DTI)- Building Technology Division- Concrete Centre provided supplementary financial support for the experimental work.

References

1. P. K. MEHTA, in "Proceedings of the 1st CANMET/ACI International Conference on the Use of Fly Ash, Silica Fume, Slag and Natural Pozzolans in Concrete," Montebello, July 1983, edited by V. M. Malhotra (ACI SP-79, Detroit, 1983) p. 1.
2. A. M. NEVILLE, "Properties of Concrete" (Longman, Essex, 1995).
3. S. BRUNAUER and L. E. COPELAND, *Scientific American* **210** (1964) 80.
4. H. M. JENNINGS, in "Advances in Cement Technology" (Pergamon Press, New York, 1983) p. 537.
5. V. JOHANSEN and N. THAULOW, in "The Modelling of Microstructure and Its Potential for Studying Transport Properties and Durability" (Kluwer Academic Publishers, Amsterdam, 1996) p. 65.
6. H. F. W. TAYLOR, in "Proceedings of the 8th International Congress on the Chemistry of Cement," Rio de Janeiro, 1986, Vol. 1, p. 82.
7. I. G. RICHARDSON and G. W. GROVES, *J. Mater. Sci.* **28** (1993) 265.
8. G. BINNING, C. F. QUATE and C. GERBER, *Phys. Rev. Lett.* **56** (1986) 930.
9. P. K. HANSMA, V. B. ELINGS, O. MARTI and C. E. BRACKER, *Science* **242** (1988) 209.
10. G. BINNING, C. GERBER, E. STOLL, T. ALBRECHT and C. F. QUATE, *Europhys. Lett.* **3** (1987) 1281.
11. T. R. ALBRECHT and C. F. QUATE, *J. Appl. Phys.* **62** (1987) 2599.
12. B. DRAKE, C. B. PRATER, A. L. WEISENHORN, S. A. C. GOULD, T. R. ALBRECHT, C. F. QUATE, D. S. CANNELL, H. G. HANSMA and P. K. HANSMA, *Science* **243** (1989) 1586.
13. C. HALL, in "Proceedings of the SPE International Symposium on Oilfield Chemistry," San Antonio, February 1995, p. 533.
14. H. UCHIKAWA, S. HANEHARA, T. SHIRASAKA and D. SAWAKI, *Cem. Concr. Res.* **22** (1992) 1115.
15. L. D. MITCHELL, M. PRICA and J. D. BIRCHALL, *J. Mater. Sci.* **31** (1996) 4207.
16. G. PAPAVALASSILIOU, M. FARDIS, E. LAGANAS, A. LEVENTIS, A. HASSANIEN, F. MILIA, A. PAPAGEORGIOU and E. CHANIOTAKIS, *J. Appl. Phys.* **82** (1997) 449.
17. C. M. DEMANET, *Appl. Surf. Sci.* **89** (1995) 97.
18. P. K. MEHTA, in "Proceedings of the 3rd CANMET/ACI International Conference on the Use of Fly Ash, Silica Fume, Slag and Natural Pozzolans in Concrete," Trondheim, June 1989, edited by V. M. Malhotra (ACI SP-114, Detroit, 1989) p. 1.
19. V. G. PAPADAKIS and E. J. PEDERSEN, in "Proceedings of the 6th CANMET/ACI International Conference on the Use of Fly Ash, Silica Fume, Slag and Natural Pozzolans in Concrete," Bangkok, June 1998, Suppl. papers, p. 355.
20. V. G. PAPADAKIS, C. G. VAYENAS and M. N. FARDIS, *ACI Mat. J.* **88** (1991) 186.

Received 28 July
and accepted 26 August 1998